Glassy carbon electrode modified with G-MoS_2-Nafion acts as an electrochemical biosensor to determine uric acid in human serum

BO YAN[1*], DONGSHENG WANG[2*], QIANG WANG[2], XIAOLAN LU[2], QIN DU[2], QI LIANG[1], XINGLIANG JIANG[2], XIAOLAN GUO[1,3], JINGGUO ZHOU[4] and YAN XING[1]

[1]Department of Laboratory Medicine, North Sichuan Medical College; [2]Department of Laboratory Medicine, Affiliated Hospital of North Sichuan Medical College; [3]Translational Medicine Center, North Sichuan Medical College; [4]Department of Rheumatology, Affiliated Hospital of North Sichuan Medical College, Nanchong, Sichuan 637000, P.R. China

Received December 22, 2017; Accepted May 22, 2018

DOI: 10.3892/mmr.2018.9314

Abstract. At present, the majority of methods used for uric acid (UA) detection are not able to meet the detection requirements with speed, accuracy, high sensitivity, high specificity, a wide linear range or a low cost. Compared with other methods, the electrochemical method has a high sensitivity and fast detection. The present study aimed to identify an electrochemical sensor with high sensitivity, fast detection and a wide linear range for the detection of UA. A glassy carbon electrode modified with graphene-molybdenum disulfide-Nafion (G-MoS_2-Nafion) composites was prepared for use as the working electrode. The morphologies and elemental compositions of the G-MoS_2 composites were characterized by field emission scanning electron microscopy, elemental distribution spectrometry and X-ray diffraction, respectively. The electrochemical behaviors were investigated by cyclic voltammetry, linear sweep voltammetry and the amperometric i-t curve (i-t). The interference of glucose, ascorbic acid and dopamine, and the accuracy and precision of the electrochemical method were subsequently evaluated. The present study identified the following: (1) Only the reduction peak of UA was detected in human serum, indicating that the method established in the present study has a high specificity for the determination of UA in human serum; (2) UA concentration has a linear correlation with current intensity ($y=0.012x+0.998$; $R^2=0.998$), wide linear range and high sensitivity (minimum detectability=13.91 μM; signal-to-noise ratio=3); (3) the values of UA content in human serum were positively proportional to the clinical results ($y=0.9802x+11.494$; $R^2=0.978$); (4) the average recovery rate of UA (95.28%) and the replicability assay of the i-t electrochemical method (coefficient of variation=2.04%), suggest that the method had a high accuracy and good precision for UA detection. Due to its characteristics of good accuracy, high sensitivity, wide linear range, good anti-interference ability and replicability, G-MoS_2-Nafion has good prospects for UA detection in the clinical setting.

Introduction

Uric acid (UA) is a metabolic product of purine. Due to the antioxidation and radical scavenging of UA, it serves an important role in the metabolic processes of humans. However, abnormal levels of UA additionally serve an important role for the occurrence and development of certain diseases, including gout, hyperuricemia, renal failure, urinary calculi, hypertension, coronary heart disease, leukemia, arthritis and Lesch-Nyhan syndrome (1,2). Therefore, a simple, rapid and accurate detection method of UA may have an important role in the diagnosis, treatment, monitoring and prevention of the aforementioned diseases.

At present, the common detection methods include enzymology, spectrophotometry, high performance liquid chromatography and electrochemical luminescence (3-5). However, these methods have the disadvantages of low sensitivity, complex detection process, a narrow linear range and high cost. In recent years, due to the advantages of high sensitivity, fast detection and low cost, electrochemical sensing methods have been widely investigated. However, the majority of the electrochemical sensors used for UA detection remain unable to avoid the disadvantages of low sensitivity, narrow linear range and poor specificity (7-9). Therefore, identifying an ideal electrochemical sensor has become a popular research focus in recent years.

In 2004, Novoselov *et al* (6) synthesized graphene for the first time. Graphene is a novel carbon nanomaterial that has a two-dimensional honeycomb crystal structure and is composed of an sp^2 hybrid monolayer of carbon atoms connected by

Correspondence to: Dr Jingguo Zhou, Department of Rheumatology, Affiliated Hospital of North Sichuan Medical College, 63 Wenhua Road, Nanchong, Sichuan 637000, P.R. China
E-mail: zhoujingguo2242@163.com

Professor Yan Xing, Department of Laboratory Medicine, North Sichuan Medical College, 234 Fujiang Road, Nanchong, Sichuan 637000, P.R. China
E-mail: xingyan2242753@163.com

*Contributed equally

Key words: uric acid, graphene, molybdenum disulfide, electrochemical biosensor

covalent bonds. This special structure has the advantages of a high specific surface area, good electrical conductivity, excellent mechanical strength and high electrocatalytic activity (10-12). Graphene has additionally been identified to have a series of other novel unique properties, including good bio-affinity, a perfect quantum tunnel effect, and room-temperature ferromagneticity (13-16). Thus, graphene has been widely used in nano-electronics, energy storage, biochemical sensors and numerous other fields in previous years (17,18). However, due its hydrophobicity, strong van der Waals forces and π-π conjugated bond interactions, the monolayer of graphene tends to aggregate and may even be converted into graphite in aqueous solution (19,20). This greatly limits the applications of graphene in electrochemical biosensors.

Molybdenum disulfide (MoS_2) is a member of the transition metal dichacogenide family. MoS_2 has a similar crystal structure, physical properties and chemical properties to graphene. The crystal structure of MoS_2 is similar to a 'sandwich' structure that is composed of 'S-Mo-S' units (21,22). The atoms are strongly connected by 'S-Mo' covalent bonds, and the triple layers are weakly connected to each other by van der Waals forces, leading to relative sliding between layers (23,24). Due to its specific surface area, strong adsorption capacity, high catalytic activity and weak interlayer-friction, MoS_2 is widely used in the manufacturing of battery electrode materials, catalysts, electrochemical devices, hydrogen storage materials and solid lubricants (25-28). Compared with graphene, the MoS_2 monolayer is not able to aggregate and has improved chemical stability in aqueous solution. However, the conductivity and structural strength of MoS_2 are far inferior to that of graphene, which additionally limits its application in the field of electrochemical biosensors (29,30).

In the present study G-MoS_2 composites were synthesized via the hydrothermal method. Due to the synergistic interaction between graphene and MoS_2, the G-MoS_2 composites have a high catalytic efficiency and electrical conductivity, in addition to avoiding the conversion of graphene into graphite in aqueous solution. The electrochemical behavior of glucose (Glu), ascorbic acid (AA), dopamine (DA), UA and human serum UA at a G-MoS_2-Nafion/glassy carbon electrode (GCE) were investigated by cyclic voltammetry (CV), linear sweep voltammetry (LSV) and amperometric i-t curve (i-t).

Materials and methods

Equipment. The following equipment was used: Electrochemical workstation (CHI-760E; Shanghai Chenghua Machinery Co., Ltd., Shanghai, China); ultrasonic cleaner (KQ-300DA; Kunshan Ultrasonic Instruments Co., Ltd., Kunshan, China); electronic balance (FA1004; Shanghai Yueping Scientific Instrument Co., Ltd., Shanghai, China); electric heating air blast drying oven (DHG-9023; Shanghai Suopu Instrument Co., Ltd. Shanghai, China; http://suopuyiqi.goepe.com/); freeze drying oven (DZF-6020; Shanghai Xinmiao Medical Equipment Manufacturing Co., Ltd., Hangzhou, China); field-emission scanning electron microscope (SEM; Low Vacuum JSM-6510; JEOL, Ltd., Tokyo, Japan); elemental distribution spectrometer (EDS; Hitachi/S-4800; Hitachi, Ltd., Tokyo, Japan); and X-ray diffractometer (XRD; Dmax/Ultima IV; Rigaku Corporation, Tokyo, Japan).

Electrochemical analysis system. Electrochemical measurements were performed with the three-electrode system (working electrode, reference electrode and auxiliary electrode) electrochemical workstation. The G-MoS_2-Nafion/GCE was used as the working electrode. A saturated calomel electrode (Ag/AgCl; C_{KCl}=3 mol/l) and a platinum wire were used as the reference and auxiliary electrodes, respectively.

Reagents. Glu, AA, DA and UA were purchased from Aladdin Biochemical Technology Ltd. (Shanghai, China). Graphite powder, H_2SO_4 (98%), $NaNO_3$, HCl (5%), H_2O_2 (30wt%), $KMnO_4$, ammonium molybdatetetrahydrate ($H_{24}Mo_7N_6O_{24}{\cdot}4H_2O$) and thioacetamide ($C_2H_5NS$) were purchased from the Chengdu Kelong Chemical Reagent Factory (Chengdu, China). Nafion solution (5%) was purchased from Sigma-Aldrich; Merck KGaA (Darmstadt, Germany). PBS (0.2 M; pH=7.4) was prepared with Na_2HPO_4 and NaH_2PO_4. Twice distilled water was used in all of the experiments. All reagents and chemicals were of analytical grade.

Patients. The human serum samples used in the present study were collected from human peripheral blood preserved by the Laboratory Department of The Affiliated Hospital of North Sichuan Medical College (Nanchong, China), between March 2017 and May 2017. A total of 35 human serum samples were collected, including 23 males and 12 females. The age distribution was in the range of 20-60 years old. As the study did not involve direct clinical studies in humans, the interests of the serum donors were not at risk of harm. With the permission of the ethical review committee of the Affiliated Hospital of North Sichuan Medical College, it was necessary to inform the individuals of the primary contents of the present study, and to ensure that the collected serum not be used in other experiments. All patients involved in the present study signed written consent agreements.

Synthesis of graphene oxide (GO). GO was synthesized from graphite powder using the modified Hummers method (31). Graphite (5 g) was added to concentrated H_2SO_4 (120 ml) under magnetic stirring at room temperature, to which $NaNO_3$ (2.5 g) was added. The mixture was maintained at 0-5˚C. Under vigorous agitation for 30 min, $KMnO_4$ (15 g) was added slowly while the temperature of the mixture solution was maintained at <20˚C. The mixed solution was incubated in a 30˚C water bath for 12 h to form a thick paste. Subsequently, 150 ml distilled water was slowly added, stirred vigorously, and allowed to react for a further 12 h in a 98˚C water bath. A volume of 50 ml H_2O_2 (30%) was added to the solution, altering the color of the solution from brown to yellow. The mixture was rinsed and centrifuged for 5 min (2,900 x g, 25˚C) with HCl (5%) and distilled water numerous times (until pH 7.0 was reached) to remove the SO_4^{2-}, $KMnO_4$ and other residual substances. The sediment was filtered out and dried in a 60˚C vacuum drying oven for 12 h. The GO was obtained as a solid black film.

Synthesis of G-MoS_2 composites. G-MoS_2 composites were prepared using the hydrothermal process (32,33). GO (60 mg) was dispersed in 20 ml distilled water by ultrasonication (60 kHz, 55˚C) for 1 h. $H_{24}Mo_7N_6O_{24}{\cdot}4H_2O$ (26.5 mg) and

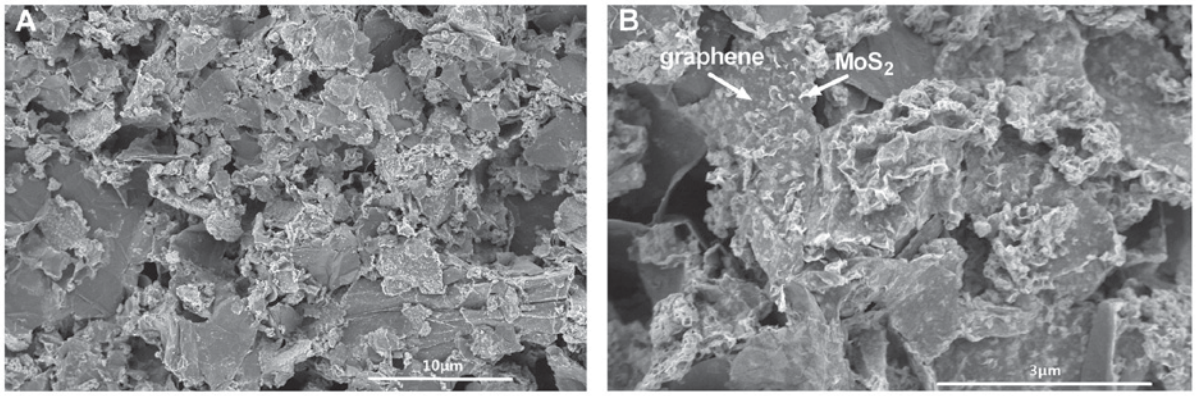

Figure 1. Scanning electron microscopy images of graphene-MoS_2 with different magnifications. (A) Magnification, x10,000; (B) magnification, x50,000. MoS_2, molybdenum disulfide.

C_2H_5NS (60 mg) were added to the GO aqueous dispersion by ultrasonication for 30 min (60 kHz, 55˚C) to form a homogeneous solution. The solution mixture was transferred to a 100-ml Teflon-lined stainless steel autoclave and heated in an electric oven at 200˚C for 24 h. The autoclave was naturally cooled to room temperature, and the black solid was obtained by filtration, rinsing and centrifugation (2,900 x g, 5 min, 25˚C) three times. The solid was subsequently dried in a -20˚C freeze-drying oven, with the obtained black solid samples denoted as G-MoS_2.

Element verification of G-MoS_2 composites. In order to verify that the G-MoS_2 composites were successfully prepared, the morphologies of G-MoS_2 composites were characterized by a Low Vacuum JSM-6510 field-emission scanning electron microscope (SEM) with platinum as the sputter coating (20 kV, $1.18x10^{-3}$ Pa, 25˚C). Briefly, 10 mg G-MoS_2 was dispersed in 10 ml absolute ethyl alcohol by ultrasonication (60 kHz, 55˚C) for 30 min. Subsequently, the sample was dripped onto a silicon wafer, dried, sprayed with platinum and detected using the SEM. The elemental compositions of G-MoS_2 composites were recorded on a Hitachi/S-4800 elemental distribution spectrometer (30 kV, dead-time: 92%) and a Rigaku Dmax/Ultima IV diffractometer with monochromatized Cu Kα radiation (Kα/λ=0.15418 nm). To verify whether the G-MoS_2 composites prepared in the present study were consistent with the standard graphene and MoS_2, the graphene of the G-MoS_2 composites was compared with a previous study (34) and MoS_2 of the G-MoS_2 composites was compared with the Powder Diffraction File card of MoS_2 [Joint Committee on Powder Diffraction Standards (JCPDS) file no. 17-744].

Preparation of the modified electrode. The GCE was sequentially polished with 1.0, 0.3 and 0.05 μm alumina slurry on velvet. The residual alumina slurry was rinsed off with distilled water, and the GCE was placed in anhydrous ethanol and distilled water with ultrasonication (60 kHz, 55˚C) for 10 min. The cleaned GCE was dried with an infrared lamp. The G-MoS_2 composite (30 mg) and Nafion solution (10 μl) were dispersed in 15 ml anhydrous ethanol with ultrasonication (60 kHz, 55˚C) for 30 min to obtain a homogenous suspension. The G-MoS_2-Nafion-modified electrode was prepared by casting 5 μl suspension onto the pretreated GCE, followed by drying with an infrared lamp.

Catalytic activity evaluation of the modified electrode. Firstly, the prepared GCE was placed in PBS (20 ml; pH=7.4) for 10 min and the CV curve of PBS was determined. The GCE was subsequently rinsed five times with distilled water and the GCE was modified with G-MoS_2-Nafion. The G-MoS_2-Nafion/GCE was placed in PBS for 2 h and the CV curve of PBS was determined. Finally, 20, 40, 60, 80 and 100 μl UA (100 mM) were added to the PBS. The resulting concentrations were 100, 200, 300, 400 and 500 μM, and their corresponding CV curves were determined.

Specificity evaluation of the modified electrode. The PBS was detected with the G-MoS_2-Nafion/GCE and a control LSV curve was obtained. Subsequently, 10 μl NaOH (1.0 M), Glu (2.0 M), AA (0.1 M), DA (0.1 M) and UA (0.1 M) were added to the PBS and the interference LSV curve was obtained.

Subsequently, an LSV assay was conducted for the human serum samples to confirm whether there may be an effect of other human serum components (including Glu, AA and DA) when detecting the UA in human serum with the G-MoS_2-Nafion/GCE. PBS was initially detected with the G-MoS_2-Nafion/GCE and a reference LSV curve was obtained. Subsequently, 4 ml PBS was removed and 4 ml of human serum was added to the PBS. The mixed solution of PBS (16 ml) and human serum (4 ml) was subsequently detected with the G-MoS_2-Nafion/GCE and the experimental LSV curve was obtained.

Quantitative detection of human serum UA with G-MoS_2-Nafion/GCE. Compared with the CV and LSV electrochemical analysis methods, i-t may be used to measure the average current values of different concentrations of UA more easily, stably and accurately. Therefore, i-t was selected to detect the UA in solution and in human serum. The G-MoS_2-Nafion/GCE was placed in PBS (20 ml) for 500 sec, and 10 μl different concentrations of UA solution were added into the PBS every 50 sec.

Methodology of the comparison analysis. The UA quantitative detection of the mixed serum was performed using a

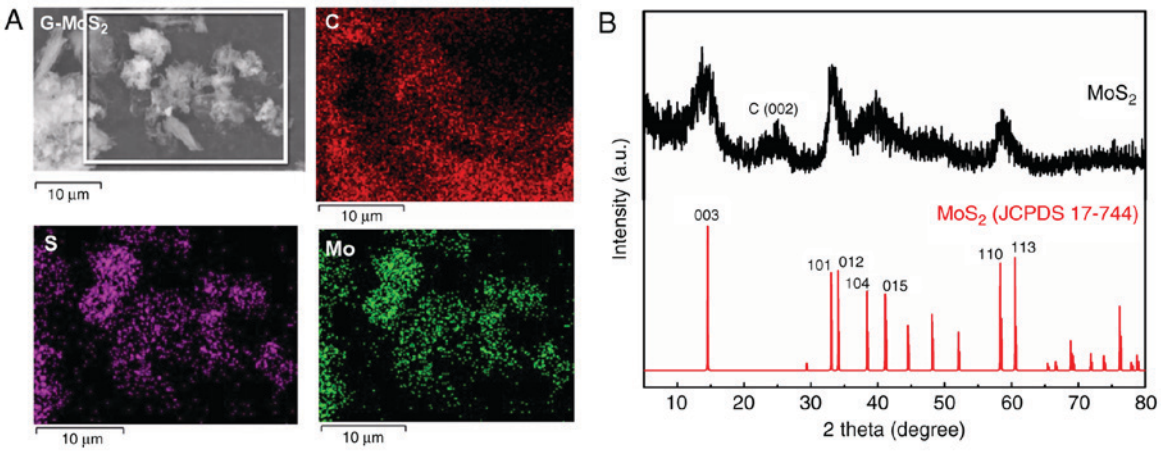

Figure 2. Verification of the elemental composition in G-MoS_2 composites. (A) Elemental distribution spectrometer analysis of G-MoS_2. (B) X-ray diffractometer analysis of G-MoS_2 (Cu Kα/λ=0.15418 nm). G-MoS_2, graphene-molybdenum disulfide; C, carbon; S, sulfur; JCPDS, Joint Committee on Powder Diffraction Standards.

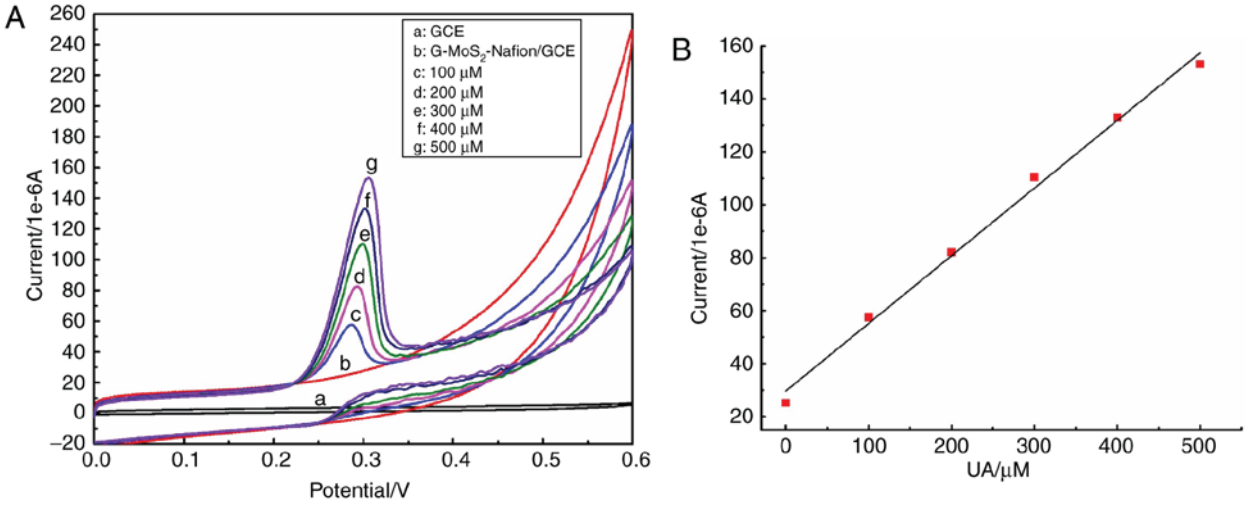

Figure 3. Evaluation of the catalytic activity of G-MoS_2-Nafion/GCE. (A) CV behavior of G-MoS_2-Nafion/GCE in different UA solution (scan rate, 0.05 V/sec). (B) The linear fitting of different UA solutions and the corresponding current values. CV, cyclic voltammetry; G-MoS_2, graphene-molybdenum disulfide; GCE, glassy carbon electrode; UA, uric acid.

uricase colorimetric assay. The G-MoS_2-Nafion/GCE was placed in PBS (16 ml) for 500 sec prior to detection of the mixed serum samples and 4 ml mixed serum was subsequently added to the PBS. The average current intensity of the mixed serum was measured. The UA concentration values of mixed serum were obtained by the conversion of the calibration curve and the linear correlation was determined. The results from UA determination using uricase colorimetric assay and G-MoS_2-Nafion/GCE were further analyzed.

Recovery and repeatability analysis of G-MoS_2-Nafion/GCE. Following measurement of the current values of the mixed serum with G-MoS_2-Nafion/GCE, a further 10 ml UA solution (100 mM) was added to the PBS immediately. The average current intensity was recorded and the total UA concentration values were obtained using the calibration curve. The MoS_2-Nafion/GCE was used to detect the UA solution (200 μM) 11 times.

Statistical analysis. All data are presented as the means ± standard deviation of three experiments. The data were analyzed using SPSS 13.0 (SPSS Inc., Chicago, IL, USA) or GraphPad Prism 5.0 (GraphPad Software, Inc., La Jolla, CA, USA). The relationship between two variables was analyzed using linear regression. Comparison of the results obtained by uricase colorimetric assay and G-MoS_2-Nafion/GCE were performed using Student's t-test and one-way analysis of variance with Dunnett's post hoc test. $P<0.05$ was considered to indicate a statistically significant difference.

The precision test results were verified using Grubbs' test. According to Grubbs' test, when the test is repeated 11 times, P=0.01 or 0.05 as long as the significance level is not greater than the critical value (Ga. n=2.484 or 2.234), indicating that the corresponding result is not an outlier. In addition, according to the Health Industry Standards of the People's Republic of China (http://www.nhfpc.gov.cn/zhuz/s9492/201301/c8dd48222ab14387a6503667be78bec3.shtml), the precision of uric acid

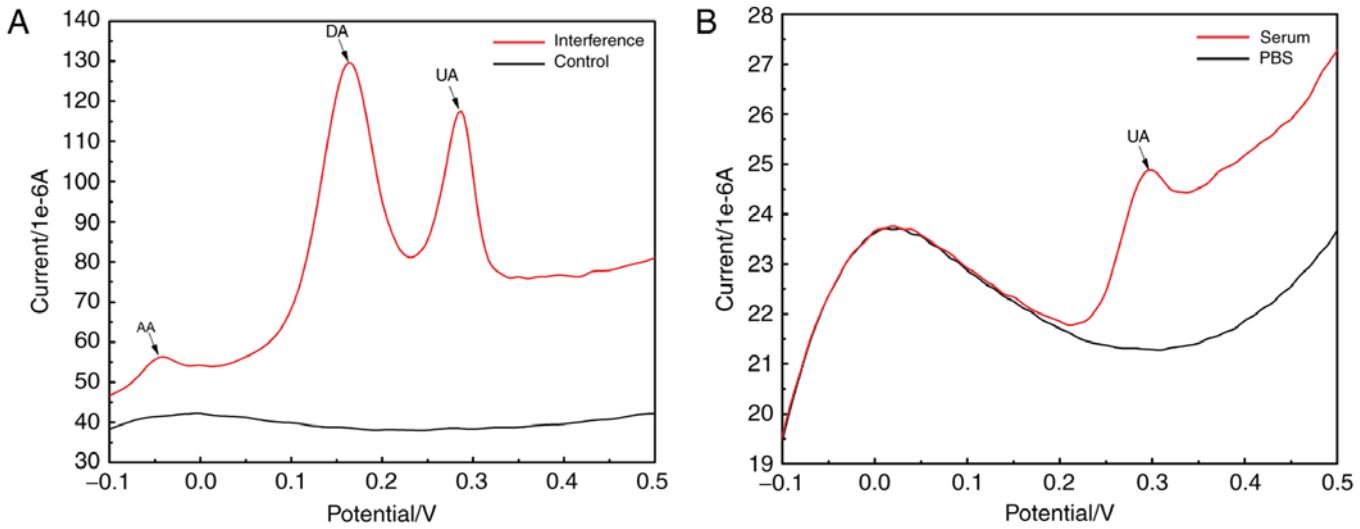

Figure 4. Interference test of the electrochemical catalytic reaction between G-MoS_2 and UA. (A) LSV electrochemical behavior of G-MoS_2-Nafion/GCE in PBS, which contains glucose, NaOH, ascorbic acid, DA and UA (scan rate, 0.1 V/sec). (B) LSV electrochemical behavior of PBS and human serum (scan rate, 0.1 V/sec). LSV, linear sweep voltammetry; G-MoS_2, graphene-molybdenum disulfide; GCE, glassy carbon electrode; DA, dopamine; UA, uric acid.

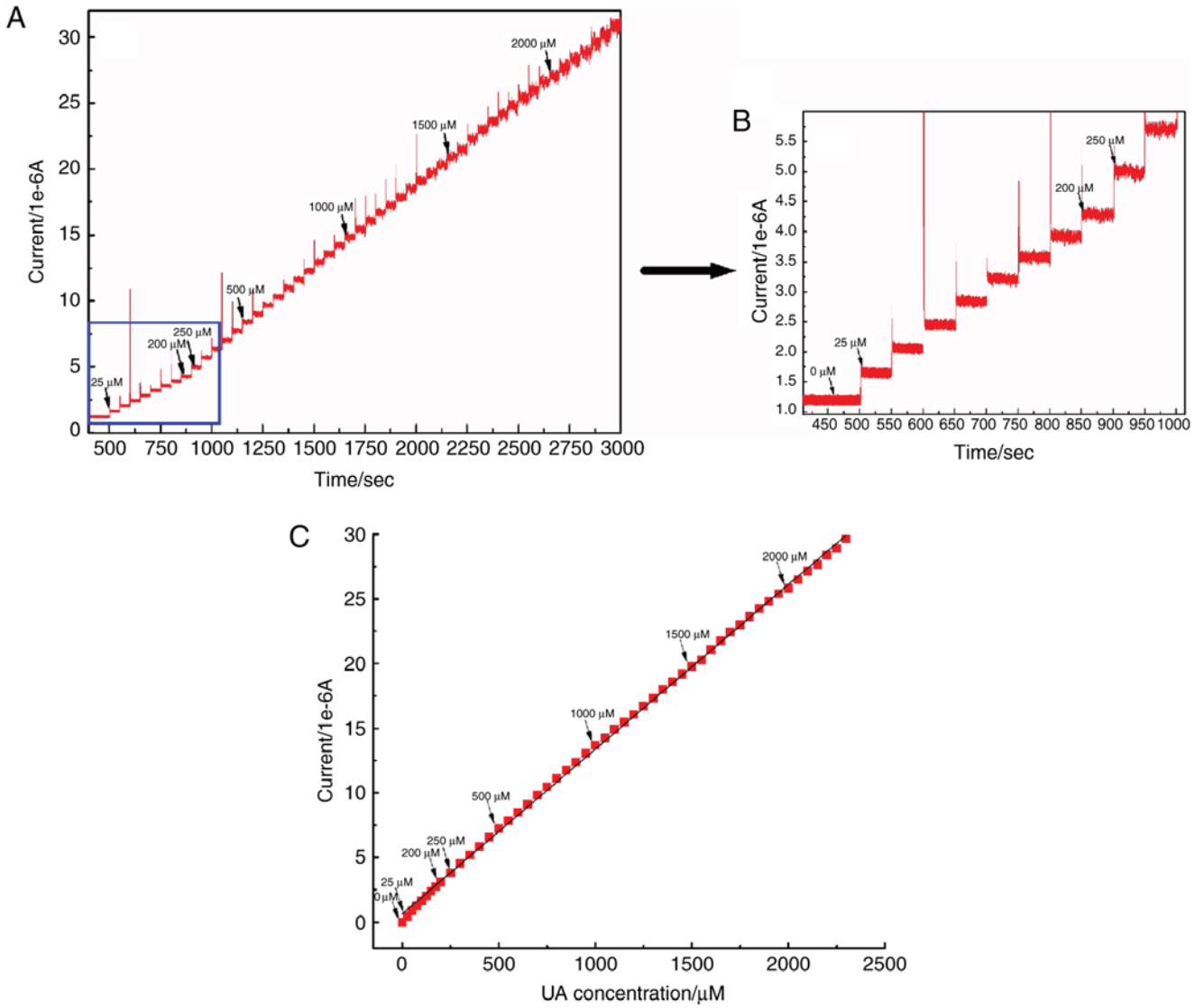

Figure 5. Calibration test for the detection of UA by G-MoS_2-Nafion/GCE. (A) I-t analysis of different concentrations of UA. (B) The local amplification image of (A). (C) The linear correlation between different concentrations of UA and their corresponding current values (y=0.012x+0.645; R^2=0.998). The minimum detectable limit was 13.91 μM (signal-to-noise ratio=3). UA, uric acid.

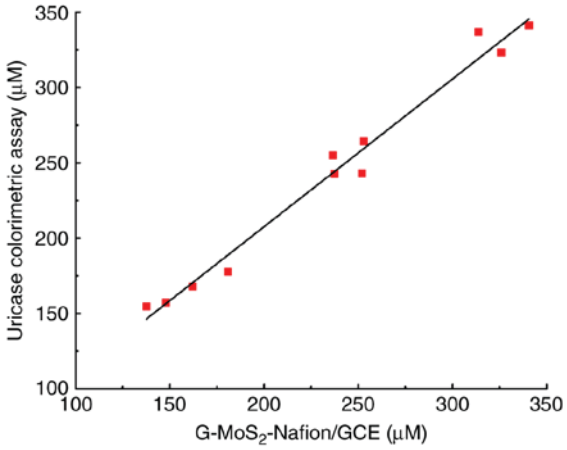

Figure 6. Linear correlation of serum uric acid concentration, which was measured by uricase colorimetric assay and G-MoS_2-Nafion/GCE, respectively (y=0.9802x+11.494; R^2=0.978). G-MoS_2, graphene-molybdenum disulfide; GCE, glassy carbon electrode.

Table I. Concentration values of serum uric acid detected by uricase colorimetric assay and G-MoS_2-Nafion/GCE (n=11).

Serum sample	Uricase colorimetric assay, μM	G-MoS_2-Nafion/GCE, μM
1	154.5	137.6
2	243.1	252.0
3	341.2	340.6
4	167.9	162.1
5	254.8	236.5
6	177.8	180.9
7	264.1	253.0
8	323.1	325.9
9	157.3	148.0
10	242.5	237.5
11	336.8	313.8

G-MoS_2, graphene-molybdenum disulfide; GCE, glassy carbon electrode.

detection is considered acceptable when the coefficient of variation <4.5%.

Results

Preparation of a good electrode modified complex. The morphology of G-MoS_2 was characterized by SEM (Fig. 1). The MoS_2 nanoparticles were densely loaded on the graphene nanosheets, and the flexible graphene nanosheets with wrinkled edges were randomly hybridized with MoS_2 nanoparticles. This structure facilitates a good connection and close contact between the graphene and MoS_2, thus increasing the contact area with the analytes.

The elemental composition of G-MoS_2 was analyzed using an EDS (Fig. 2A). The carbon elements of graphene were evenly distributed on the graphene nanosheets. The molybdenum elements and sulfur elements of MoS_2 were distributed in the corresponding positions of MoS_2 nanoparticles, and the G-MoS_2 composite contained no other elements except carbon, molybdenum and sulfur. This indicated that G-MoS_2 composites were successfully synthesized.

XRD testing was conducted to examine the crystalline characteristics of G-MoS_2 (Fig. 2B). The characteristic diffraction peak of graphene may be identified at 25˚, which corresponds to C (002), and this is consistent with a previous study (34). The MoS_2 demonstrated its characteristic diffraction peaks when compared with the Powder Diffraction File card of MoS_2 (JCPDS file no. 17-744) and no other miscellaneous peaks were observed. The diffraction peaks of MoS_2 at 14.5, 32.8, 34.2, 38.2, 41.1, 58.2 and 60.4˚, were consistent with the (003), (101), (012), (104), (015), (110) and (113) crystal planes of MoS_2 (JCPDS file no. 17-744), respectively, indicating that the G-MoS_2 composites synthesized in the present study contained a high purity of graphene and MoS_2.

G-MoS_2-Nafion/GCE has a good electrochemical catalytic activity for UA. The electrochemical catalytic activity of the G-MoS_2-Nafion/GCE with the addition of different concentrations of UA was assessed (Fig. 3A). No current intensity alteration or any characteristic peak was observed in the CV curve 'a', which was within the potential range of 0-0.6 V, suggesting that no electrochemical reaction occurred on the GCE alone. An increased current intensity was observed in the CV curve 'b'; however, no oxidation or reduction peak was observed, indicating that although the conductivity of the G-MoS_2-Nafion/GCE was enhanced compared with the naked GCE, there was no electrochemical reaction occurring on the G-MoS_2-Nafion/GCE. When different concentrations of UA were added into PBS, reduction peaks appeared between 0.28 and 0.32 V, and the reduction current intensity increased gradually as the concentration of UA increased in PBS. As there were no marked oxidation peaks in the CV curves of 'c-g', it suggested that electrochemical catalytic activity of UA occurring on the G-MoS_2-Nafion/GCE could be monitored.

When the UA concentration was fitted with the corresponding current intensity, as demonstrated in Fig. 3B, the oxidation current intensity increased with the enhancement of the UA concentration, exhibiting a strong linear correlation (y=0.256x+29.63; R^2=0.9931).

AA, DA and other components did not interfere with the electrochemical catalytic reaction between G-MoS_2 and UA. Fig. 4A demonstrated that only electrochemical oxidation reactions of AA, DA and UA occurred at the G-MoS_2-Nafion/GCE, and the corresponding potential values of their reduction peaks are -0.04, 0.16 and 0.29 V, which suggests that the reduction peaks of AA, DA and UA were distinct from each other. The reduction peak current intensities of DA and UA were markedly higher compared with AA. Nafion may enhance the adhesion of G-MoS_2 composites on the GCE surface, extend the G-MoS_2-Nafion/GCE service life and have a shielding effect towards the anion. Therefore, the Nafion may significantly reduce the electrochemical oxidation reaction of AA that occurs on the G-MoS_2-Nafion/GCE (35).

Table II. Recovery rate of serum uric acid measured by graphene-molybdenum disulfide-Nafion/glassy carbon electrode (n=11).

Serum sample	Basic found, μM	Added, μM	Total found, μM	Recovery value[a], μM	Recovery rate[b], %
1	137.6	200.0	324.2	186.6	93.3
2	252.0	200.0	448.0	196.0	98.0
3	340.6	200.0	536.6	196.0	98.0
4	162.1	200.0	345.5	183.4	91.7
5	236.5	200.0	427.1	190.6	95.3
6	180.9	200.0	371.1	190.2	95.1
7	253.0	200.0	443.0	190.0	95.0
8	325.9	200.0	518.9	193.0	96.5
9	148.0	200.0	334.8	186.8	93.4
10	237.5	200.0	428.5	191.0	95.5
11	313.8	200.0	506.4	192.6	96.3
Average value	-	-	-	190.56	95.28

[a]Recovery value = Total found - Basic found. [b]Recovery rate = 100 x Recovery value/Added.

As shown in Fig. 4B, only the UA reduction peak (potential, 0.29 V) was observed, and no other marked reduction peaks were observed at the potential locations of AA (-0.04 V) or DA (0.16 V) compared with the reference LSV curve. This indicates that the G-MoS_2-Nafion/GCE had a good selectivity for the determination of UA in human serum.

G-MoS_2-Nafion/GCE has a good performance for the determination of UA. The calibration i-t curve of UA is demonstrated in Fig. 5A. With each addition of UA (50 μM) an obvious and uniform current change was observed on the i-t curve (Fig. 5B). The linear correlation between different concentrations of UA and their corresponding current values is demonstrated in Fig. 5C.

As indicated in Fig. 5 that the current values increased with an increase in the UA concentration, and there was a linear correlation between them (y=0.012x+0.645; R^2=0.998). Furthermore, the minimum detectable value was 13.91 μM (signal-to-noise ratio: S/N=3), and the linear correlation between the concentration of UA and current values was between 25 and 3,000 mM. This suggested that G-MoS_2-Nafion/GCE had a high sensitivity and wide linear range for the determination of UA.

Serum UA determined by uricase colorimetric assay and G-MoS_2-Nafion/GCE have a high degree of correlation. The UA concentration of the mixed serum was detected by a uricase colorimetric assay and G-MoS_2-Nafion/GCE (Table I). The correlation between the two methods is shown in Fig. 6, which demonstrated that there was a good linear correlation between them (y=0.9802x+11.494; R^2=0.978).

Detection of UA by G-MoS_2-Nafion/GCE is accurate and precise. In order to verify the accuracy and precision of using the working electrode prepared in the present study to detect human serum UA, recovery and repeatability analysis was conducted, respectively. As shown in Table II, with an average recovery rate of 95.28%, G-MoS_2-Nafion/GCE had a high accuracy for the detection of UA. Therefore, as demonstrated in Table III, no outlier value existed in the present study. Furthermore, the coefficient of variation was 2.04% (<4.5%), which suggested that the G-MoS_2-Nafion/GCE used in the present study also had an acceptable precision for UA determination.

Table III. Precision analysis of UA detected by graphene-molybdenum disulfide-Nafion/glassy carbon electrode (n=11).

Test no.	UA value, μM	Significance level
1	186.6	1.02
2	196.0	1.40
3	196.0	1.40
4	183.4	1.84
5	190.6	0.01
6	190.2	0.09
7	190.0	0.14
8	193.0	0.63
9	186.8	0.97
10	191.0	0.11
11	192.6	0.52
Average value	190.56	-
SD	3.89	-
CV (100%)	2.04	-

Significance level = |UA value - Average valuel/SD. CV, coefficient of variation; SD, standard deviation; UA, uric acid.

Discussion

At present, the primary methods of preparing GO include the improved Hummers, Brodie and Staudenmaier methods (36-38). The modified Hummers method, used in the present study, is one of the most important methods of

preparing GO due to its advantages, including a simple and fast reaction process, and a safer operation compared with other methods. The GO synthesized using the improved Hummers method is rich in oxygen-containing functional groups that contribute to the complex structure of GO. This special structure is beneficial to allow graphene to combine closely with other materials.

The primary methods used for G-MoS_2 synthesis include three types of methods: Hydrothermal synthesis; chemical vaporous deposition; and automatic liquid assembly (39-41). The hydrothermal synthesis method, which was used in the present study, is an effective method of synthesizing a more compact structure of G-MoS_2. This method additionally has the advantages of mild reaction conditions, simple operation, less environmental pollution and low cost, and the morphology of the synthetic materials may be controlled easily. The morphology, size and structure of the materials may be controlled by altering the conditions of the reaction (42). Under conditions of high temperature and high pressure, due to the effect of electrostatic attraction, the molybdate is adsorbed onto the surface of GO and reacts with sulfur to form MoS_2. Simultaneously, the GO is additionally reduced and transformed into graphene by removing its oxygen-containing groups gradually, and the graphene continues to react with MoS_2 to form G-MoS_2 composites (43,44). In this reaction process, GO acts as a template for the hydrothermal reaction. It provides a good foundation for improving the compactness, avoiding defects and preserving the advantages of MoS_2 and graphite.

Based on the above principles, the improved Hummers and hydrothermal synthesis methods were selected in the present study to prepare an electrochemical biosensor, which was derived from the graphite and MoS_2 composite, for the determination of UA in human serum. The present study suggested that the G-MoS_2-Nafion/GCE had catalytic oxidation activity towards AA, DA and UA; however, the catalytic efficiencies for UA and DA were markedly improved compared with AA. Nafion may not enhance the adhesion of G-MoS_2 composites, and may additionally restrain the oxidation or reduction reactions of negatively charged substances, including AA, at the G-MoS_2-Nafion/GCE surface.

The present study demonstrated that the reduction peaks of AA, DA and UA may be well-separated, and only the UA reduction peak was detected by the G-MoS_2-Nafion/GCE in the human serum samples. This suggested that the method had high specificity for the determination of UA in human serum. Furthermore, the UA concentration had a linear correlation with its corresponding current intensity, a wide linear range and a high sensitivity (the minimum detectable value was 13.91 μM; S/N=3) for the determination of UA. The values of human serum UA, measured using the G-MoS_2-Nafion/GCE and an uricase colorimetric assay, had a positive correlation. The average recovery rate of UA detected with G-MoS_2-Nafion/GCE was 95.28%, indicating that the electrochemical method used in the present study had a high accuracy for the detection of UA. Additionally, the repeatability tests demonstrated that the electrochemical method had a high precision for the detection of UA.

Although an electrode modifier for serum UA detection was successfully identified, there remain certain limitations to the present research. The feasibility of G-MoS_2-Nafion/GCE for the detection of human serum UA was analyzed; however, the specific electrochemical catalytic reaction of UA at the G-MoS_2-Nafion/GCE electrode was not discussed. Additionally, the different LSV curves of human serum samples and mixed PBS solutions, which contained AA, DA and UA, in the feasibility analysis may be further examined in future studies. The number of mixed serum samples tested in the comparative analysis of serum UA by uricase colorimetric assay and i-t electrochemical method was low (only 11 cases). Furthermore, the concentration range of serum UA was slightly narrow in the present study. The average recovery rate of UA detected using the G-MoS_2-Nafion/GCE was <100%, suggesting that there was a systemic error in the method. The systemic error may be caused by the fact that the G-MoS_2-Nafion in the present study was a laboratory-synthesized composite, thus the dampening effect on the electrochemical catalytic ability was unavoidable. In addition, the equivalent amount of UA was added in the recovery analysis, thus, the accuracy of the analysis of the G-MoS_2-Nafion/GCE may not be verified in numerous directions. Finally, there was only one concentration of UA standard solution selected in the precision analysis, which does not cover all of the low, medium and high concentrations. Additionally, the number of repeated measurements was <20, thus the precision of the G-MoS_2-Nafion/GCE may not be fully verified at present. Therefore, improvements to the experiments to evaluate the performance of the G-MoS_2-Nafion/GCE for the detection of human serum UA is required in future studies.

Nafion, which was contained in the G-MoS_2-Nafion composites, may inhibit the electrochemical reduction reaction of AA. Therefore, it may be speculated that if another material was identified that had the ability to enhance the adhesion of G-MoS_2, and to not affect the catalytic efficiency of G-MoS_2 composites towards AA, DA and UA, the simultaneous detection of AA, DA and UA may be possible in the future.

In conclusion, the present study indicated that G-MoS_2-Nafion composites may be used as an electrochemical catalytic material for the detection of UA in human serum. Compared with other methods for the determination of UA (including enzymology, points spectrophotometry, high performance liquid phase chromatography and electrochemical chemiluminescence analysis), it has the characteristics of accuracy, high sensitivity, a wide linear range, fast detection, strong anti-interference properties, low cost, a simple preparation process, reusability and being environmentally friendly. Furthermore, human serum samples may be measured immediately without any other treatment following centrifugation. Therefore, the G-MoS_2-Nafion composite or its improved analogs as electrochemical catalysts for the determination of human serum UA has good clinical application prospects.

Acknowledgements

The authors thank Professor Jing Jiang from China West Normal University (Nanchong, China) for his assistance with the data analysis.

Funding

The present study was supported by grants from The National Natural Science Foundation of China (grant no. 81641096), the

Department of Science and Technology of Sichuan Province (grant no. 2016JY0171) and International S&T Cooperation Program of China (grant no. 2015DFA30420).

Availability of data and materials

The datasets used and/or analyzed during the current study are available from the corresponding author on reasonable request.

Authors' contributions

BY and DW designed the research and drafted the manuscript. XL and QD acquired, analyzed and interpreted the data, and performed statistical analysis. QW and QL prepared the figures. XJ and JZ diagnosed the patients and provided treatment information of hyperuricemia, and also helped improve the experimental design. XG and YX performed the element verification of G-MoS2 composites and revised the manuscript for important intellectual content. All authors read and approved the final manuscript.

Ethics approval and consent to participate

The present study was approved by the Ethics Committee of the Affiliated Hospital of North Sichuan Medical College (Nanchong, China). Written informed consent was obtained from all patients.

Patient consent for publication

All patients involved in the present study provided consent for publication.

Competing interests

The authors declare that they have no competing interests.

References

1. Popa E, Kubota Y, Tryk DA and Fujishima A: Selective voltammetric and amperometric detection of uric acid with oxidized diamond film electrodes. Anal Chem 72: 1724-1727, 2000.
2. Cardoso AS, Gonzaga NC, Medeiros CC and Carvalho DF: Association of uric acid levels with components of metabolic syndrome and non-alcoholic fatty liver disease in overweight or obese children and adolescents. Pediatr 89: 412-418, 2013.
3. Gabison L, Chiadmi M, Colloc'h N, Castro B, El Hajji M and Prangé T: Recapture of [S]-allantoin, the product of the two-step degradation of uric acid, by urate oxidase. FEBS Lett 580: 2087-2091, 2006.
4. Filisetti-Cozzi TM and Carpita NC: Measurement of uric acids without interference from neutral sugars. Anal Biochem 197: 157-162, 1991.
5. Inoue K, Namiki T, Iwasaki Y, Yoshimura Y and Nakazawa H: Determination of uric acid in human saliva by high-performance liquid chromatography with amperometric electrochemical detection. J Chromatogr B Analyt Technol Biomed Life Sci 785: 57-63, 2003.
6. Novoselov KS, Geim AK, Morozov SV, Jiang D, Zhang Y, Dubonos SV, Grigorieva IV and Firsov AA: Electric field effect in atomically thin carbon films. Science 306: 666-669, 2004.
7. Sun CC, Luo FF, Wei L, Lei M, Li GF, Liu ZL, LE WD and Xu PY: Association of serum uric acid levels with the progression of Parkinson's disease in Chinese patients. Chin Med J (Engl) 125: 583-587, 2012.
8. Li S, Qian T, Wu S and Shen J: Controllable fabrication of polystyrene/graphene core-shell microspheres and its application in high-performance electrocatalysis. Chem Commun (Camb) 48: 7997-7999, 2012.
9. Zen JM and Chen PJ: A selective voltammetric method for uric acid and dopamine detection using clay-modified electrodes. Anal. Chem 69: 5087-5093, 1997.
10. Geim AK and Novoselov KS: The rise of grapheme. Nat Mater 6: 183-191, 2007.
11. Service RF: Carbon sheets an atom thick give rise to graphene dreams. Science 324: 875-877, 2009.
12. Kim KS, Zhao Y, Jang H, Lee SY, Kim JM, Kim KS, Ahn JH, Kim P, Choi JY and Hong BH: Large-scale pattern growth of graphene films for stretchable transparent electrodes. Nature 457: 706-710, 2009.
13. Lee C, Wei X, Kysar JW and Hone J: Measurement of the elastic properties and intrinsic strength of monolayer graphene. Science 321: 385-388, 2008.
14. Chen JH, Jang C, Xiao S, Ishigami M and Fuhrer MS: Intrinsic and extrinsic performance limits of graphene devices on SiO_2. Nat Nanotechnol 3: 206-209, 2008.
15. Balandin AA, Ghosh S, Bao W, Calizo I, Teweldebrhan D, Miao F and Lau CN: Superior thermal conductivity of single-layer graphene. Nano Lett 8: 902-907, 2008.
16. Wang Y, Huang Y, Song Y, Zhang X, Ma Y, Liang J and Chen Y: Room-temperature ferromagnetism of graphene. Nano Lett 9: 220-224, 2009.
17. Stepnowski P, Müller A, Behrend P, Ranke J, Hoffmann J and Jastorff B: Reversed-phase liquid chromatographic method for the determination of selected room-temperature ionic liquid cations. J Chromatogr A 993: 173-178, 2003.
18. Ruiz-Angel MJ and Berthod A: Reversed phase liquid chromatography of alkyl-imidazolium ionic liquids. J Chromatogr A 1113: 101-108, 2006.
19. Yang H, Zhang Q, Shan C, Li F, Han D and Niu L: Stable, conduetive supramolecular composite of graphene sheets with conjugated polyelectrolyte. Langmuir 26: 6708-6712, 2010.
20. Niyogi S, Bekyarova E, Itkis ME, McWilliams JL, Hamon MA and Haddon RC: Solution properties of graphite and graphene. Am Chem Soc 128: 7720-7721, 2006.
21. Liu WW and Wang JN: Direct exfoliation of graphene in organic solvents with addition of NaOH. Chem Commun 47: 6888-6890, 2011.
22. Balendhran S, Ou JZ, Bhaskaran M, Sriram S, Ippolito S, Vasic Z, Kats E, Bhargava S, Zhuiykov S and Kalantar-Zadeh K: Atomically thin layers of MoS_2 via a two step thermal evaporation-exfoliation method. Nanoscale 4: 461-466, 2012.
23. Stephenson T, Li Z, Olsen B and Mitlin D: Lithium ion battery applications of molybdenum disulfide (MoS_2) nanocomposites. Energ Environ Sci 7: 209-231, 2014.
24. Viemeusel B, Schneider T, Tremmel S, Wartzack S and Gradt T: Humidity resistant MoS_2 coatings deposited by unbalanced magnetron sputtering. Surf Coat Tech 235: 97-107, 2013.
25. Viet Hung pHam, Kwang-Hyun Kim, Dong-won Jung, Pham VH, Kim KH, Jung DW, Singh K, Oh ES and Chung JS: Liquid phase co-exfoliated MoS_2-graphene composites as anode materials for lithium ion batteries. J Power Sources 244: 280-286, 2013.
26. Sun MY, Adjaye J and Nelson AE: Theoretical investigations of the structures and properties of molybdenum-based sulfide catalysts. Applied Catalysis A 263: 131-143, 2004.
27. Chen J, Kuriyama N, Yuan H, Takeshita HT and Sakai T: Electrochemical hydrogen storage in MoS_2 nanotubes. J Am Chem Soc 123: 11813-11814, 2001.
28. Hua KH, Hua XG and Sun XJ: MorpHological effect of MoS_2 nanoparticles on catalytic oxidation and vacuum lubrication. Applied Sur Sci 256: 2517-2523, 2010.
29. Xiao J, Choi DW, Cosimbescu L, Koech P, Liu J and Lemmon JP: Exfoliated MoS_2 nanocomposite as an anode material for lithium ion batteries. Chem. Mater 22: 4522-4524, 2010.
30. Du G, Guo Z, Wang S, Zeng R, Chen Z and Liu H: Superior stability and high capacity of restacked molybdenum disulfide as anode material for lithium ion batteries. Chem Commun (Camb) 46: 1106-1108, 2010.
31. Chen CM, Yang QH, Yang YG, Lv W, Wen Y, Hou PX, Wang M, Cheng HM: Self-assembled free-standing graphite oxide membrane. Adv Mater 21: 3007-3011, 2009.
32. Y Li, Wang H, Xie L, Liang Y, Hong G and Dai H: MoS_2 nanoparticles grown on graphene: An advanced catalyst for the hydrogen evolution reaction. J Am Chem Soc 133: 7296-7299, 2011.
33. Wang X, Zhang Z and Chen Y: Morphology-controlled synthesis of MoS_2 nanostructures with different lithium storage properties. J All Comp 600: 84-89, 2014.

34. Li XY, Ai LH and Jiang J: Nanoscale zerovalent iron decorated on graphene nanosheets for Cr(VI) removal from aqueous solution: Surface corrosion retard induced the enhanced performance. Chem Eng J 288: 789-797, 2015.
35. Szentimay MN and Martin CR: Ion-exchange selectivity of nafion films on electrode surfaces. Anal Chem 56: 1898-1902, 1984.
36. Hummers WS and Offeman RE: Preparation of graphitic oxide. Am Chem Soc 80: 1339, 1958.
37. Brodie BC: Bibiographic notices. Doublic J Mecical Sci 22: 351-379, 1855.
38. Staudenmaier L: Verfahren zur darstellung der Graphitsaure. Berichte der deutschen chemischen Gesellschaft 31: 1481-1487, 1898.
39. Yu L, Lee YH, Ling X, Santos EJ, Shin YC, Lin Y, Dubey M, Kaxiras E, Kong J, Wang H and Palacios T: Graphene/MoS_2 hybrid technology for large-scale two-dimensional electronics. Nano Lett 14: 3055-3063, 2014.
40. Jiang JW and Park HS: Mechanical properties of MoS_2/graphene heterostructures. App Phy Lett 105: 033-108, 2014.
41. Nengjie H, Kang J, Wei Z, Li SS, Li J and Wei SH: Novel and Enhanced Optoelectronic Performances of multilayer MoS_2-WS2heterostructure transistors. Adv Fun Mat 24: 7025-7031, 2014.
42. Meng F, Li J and Cushing SK: Solar hydrogen generation by nanoscale p-n junction of p-type molybdenum disulfide/n-type nitrogen-doped reduced graphene oxide. J Am Chem Soc 135: 10286-10289, 2013.
43. Chang K and Chen W: In situ synthesis of MoS_2/graphene nanosheet composites with extraordinarily high electrochemical performance for lithium ion batteries. Chem Commun 47: 4252-4254, 2011.
44. Wang Z, Chen T, Chen W, Chang K, Ma L, Huang G, Chen D and JM: CTAB-assisted synthesis of single-layer MoS_2-graphene composites as anode materials of Li-ion batteries. J Mat Chem A 1: 2202-2210, 2013.